Available online at www.sciencedirect.com
SCIENCE DIRECT®
Applied Catalysis B: Environmental 49 (2004) 73–81
APPLIED CATALYSIS B: ENVIRONMENTAL
www.elsevier.com/locate/apcatb

Effect of synthesis procedure on the low-temperature WGS activity of Au/ceria catalysts

T. Tabakova [a,*], F. Boccuzzi [b], M. Manzoli [b], J.W. Sobczak [c], V. Idakiev [a], D. Andreeva [a]

[a] *Institute of Catalysis, Bulgarian Academy of Sciences, Acad. G. Bonchev Str., bl. 11, 1113 Sofia, Bulgaria*
[b] *Department of Chemistry IFM, University of Torino, via Pietro Giuria 7, 10125 Torino, Italy*
[c] *Institute of Physical Chemistry, Polish Academy of Science, ul. Kasprzaka 44/52, 01-224 Warsaw, Poland*

Received 10 August 2003; received in revised form 24 November 2003; accepted 24 November 2003

Abstract

Gold/ceria catalysts were prepared by two different methods (deposition-precipitation and modified deposition-precipitation). Considerable differences in the low-temperature water-gas shift (WGS) activity of both catalysts were observed. The preparation technique strongly influenced catalytic activity due to the large differences in gold particles size and to the availability of active gold sites in close contact with ceria defects on the surface. HRTEM and EDS have shown presence of very highly dispersed gold clusters (d about 1 nm) on the surface of the catalyst prepared by deposition-precipitation. Large gold particles (average $d \approx 15$ nm) have been found in gold/ceria catalyst prepared by modified deposition-precipitation. FTIR spectroscopy of adsorbed CO and X-ray photoelectron spectroscopy were employed to obtain information about the surface structure of both catalysts and to explain the differences in catalytic activity.

Keywords: Gold/ceria catalyst; Water-gas shift activity; FTIR; XPS

1. Introduction

Recently, there has been considerable interest in water-gas shift (WGS) reaction because it plays a key role in the automobile exhaust processes by converting CO with water to hydrogen and CO_2 and by including the produced hydrogen as an effective reductant for NO_x removal. On the other hand, WGS reaction provides pathway to the production of pure hydrogen that can be employed in fuel-cell power systems. The replacement of the internal combustion engine in cars, motorcycles, tracks, buses, etc. with fuel-cells is a way to provide a realistic solution of environmental protection.

Gold-based catalysts have received great attention since Haruta et al. have discovered that gold exhibits surprisingly high catalytic activity for CO oxidation at temperature as low as 200 K when it is deposited as nanoparticles on metal oxides [1,2]. The increased interest and rapidly growing number of investigations on supported nano-gold catalysts is due to their potential applicability to many reactions of both environmental and industrial relevance [3–5]. The synthesis of nanosized gold catalysts is highly sensitive towards the preparation technique which determines a great difference in the size of gold particles and in their interaction with the support. Haruta and co-workers have shown that the incipient wetness impregnation is unsuitable to produce highly dispersed gold catalysts. They have developed four techniques that allow to deposit gold nanoparticles on certain metal oxides: co-precipitation (CP), co-sputtering, deposition-precipitation (DP) and gas-phase grafting [5]. In addition to these methods, combustion [6] and liquid phase grafting are also used. Studies by Iwasawa and co-workers [7] have shown that highly active gold catalysts can also be synthesized by interaction of an Au–phosphine complex with as-prepared wet metal hydroxide supports. Grunwaldt et al. have prepared active gold catalysts for CO oxidation by immobilizing gold colloids with a size of about 2 nm on TiO_2 and ZrO_2 [8].

The nature of the support on which nanosized gold particles are dispersed plays a crucial role in determining the catalytic activity. Ceria is a very suitable support for WGS catalysts. It is extensively employed as a component in the

* Corresponding author. Tel.: +359-2-9792528; fax: +359-2-9712967.
E-mail address: tabakova@ic.bas.bg (T. Tabakova).

0926-3373/$ – see front matter © 2004 Elsevier B.V. All rights reserved.
doi:10.1016/j.apcatb.2003.11.014

automobile three-way catalysts due to its ability to undergo deep and rapid reduction–oxidation cycles depending on the changes in the redox potential of the exhaust gases. Ceria is also known to stabilize the active phase in a finely dispersed state. A very good WGS activity of noble (Pt, Pd, Rh) and transition (Cu, Ni) metal-modified ceria has been already shown [9,10]. We have recently reported that deposition of gold on ceria leads not only to a high WGS activity; for the first time high stability over a long-term test was recorded for this type of gold-containing catalysts [11]. Fu et al. prepared Au-(La-doped)ceria catalysts using different techniques: co-precipitation, deposition-precipitation and urea gelation/co-precipitation [12,13]. They have found high WGS activity and stability of gold/ceria catalysts, as well. More recently, Scire et al. have reported that gold/ceria catalysts prepared by co-precipitation and deposition-precipitation present high activity towards the catalytic oxidation of VOCs [14].

In this study we investigated the effect of two different preparation techniques on the low-temperature WGS activity of Au/ceria catalysts. HRTEM, X-ray diffraction (XRD), FTIR of adsorbed CO at 90 and 300 K before and after WGS reaction, and XPS were employed to obtain information about the surface and the bulk structure of both catalysts and to explain the differences observed in the catalytic activity.

2. Experimental

2.1. Catalyst preparation

Two preparation procedures were used: deposition precipitation (DP) and a modified version of deposition-precipitation (MDP). The samples were synthesized in a "Contalab" laboratory reactor (Contraves AG, Switzerland) enabling complete control of the reaction parameters: pH, temperature, stirrer speed, reactant feed flow, etc. In the case of DP method, gold hydroxide was deposited at constant pH 7.0 and at 333 K on ceria support previously prepared by precipitation of $Ce(NO_3)_3{\cdot}6H_2O$ with K_2CO_3 at pH 9.0 and at 333 K, dried, calcined in air at 673 K for 2 h and suspended in water by ultrasound. As for the MDP method, $HAuCl_4$ was precipitated with K_2CO_3 in the same experimental conditions reported above, but the deposition of gold hydroxide was carried out on freshly prepared $Ce(OH)_3$, only aged at 333 K for 1 h. The resulting precipitates were aged in a course of 1 h at 333 K, then filtered and washed until no Cl^- or NO_3^- could be detected. Further, the precipitates were dried in vacuum at 353 K and calcined in air at 673 K for 2 h. The measured gold loading is 3 wt.%. "Analytical grade" chemicals were used in the catalyst preparation. The samples here investigated were denoted as AuCeDP for the sample prepared by deposition-precipitation and AuCeMDP for the one prepared by modified deposition-precipitation.

2.2. Catalyst characterization

HRTEM analysis was performed using a Jeol JEM 2010 (200 kV) microscope equipped with an EDS analytical system Oxford Link. The powdered samples were ultrasonically dispersed in isopropyl alcohol and the obtained suspensions were deposited on a copper grid, coated with a porous carbon film.

X-ray diffraction patterns were obtained on a DRON-3 automatic powder diffractometer (Russia), using Cu Kα1 radiation.

X-ray photoelectron data were recorded on a VG Scientific ESCALAB-210 spectrometer using unmonochromatized Mg Kα radiation (1253.6 eV) from an X-ray source operating at 15 kV and 20 mA. The binding energy scale of the spectrometer was calibrated by setting the Ag $3d_{5/2}$ peak of sputtered Ag foil to 368.27 eV. Working pressure was below 8×10^{-9} mbar. Hemispherical analyzer works at constant pass energy = 20 eV for regions Au 4f, O 1s, Ce 3d, C 1s and VB. All spectra were recorded at a photoelectron take-off angle of 90°. Charging effects were corrected by using as reference the Ce $3d_{3/2}$ u‴ line at 917.00 eV [15]. The samples were prepared as pellets and reduced "in situ" in a preparation chamber. Data processing, involved smoothing, satellite removing, nonlinear Shirley type background subtraction and curve fitting procedure, based on mixed Gaussian–Lorentzian function were done using VG ECLIPSE software. Quantitative calculations were made using MULTILINE program [16].

The FTIR absorbance spectra have been collected on a Perkin-Elmer 1760 spectrometer equipped with a MCT detector, with the sample in self-supporting pellet introduced in a cell allowing thermal treatments in controlled atmospheres and spectrum scanning at controlled temperatures (from 90 up to 300 K). The experiments were performed on the sample preliminarily heated up to 673 K in dry oxygen and cooled down in the same atmosphere (oxidized sample) or reduced in hydrogen at 523 K, cooled down in hydrogen and finally outgassed at RT (reduced sample). Band integration and curve fitting have been carried out by "Curvefit", in Spectra Calc (Galactic Industries Co.) by means of Lorentzian curves.

2.3. Catalytic activity measurements

Catalytic activity measurements were carried out in a flow reactor at atmospheric pressure over a wide temperature range (423–623 K). The following conditions were applied: catalyst bed volume 0.5 cm^3 (0.63−0.80 mm pellets), space velocity 4000 h^{-1}, and partial pressure of water vapour −31.1 kPa. The reactant gas mixture feed into the reactor contained 4.498 vol.% CO, the rest being argon. The catalysts employed for the measures were undergone to a reduction treatment for 1 h in a 1% H_2/Ar mixture at different temperatures: AuCeDP at 373 K and AuCeMDP at 423 K in accordance with TPR data. Analysis of the converted mix-

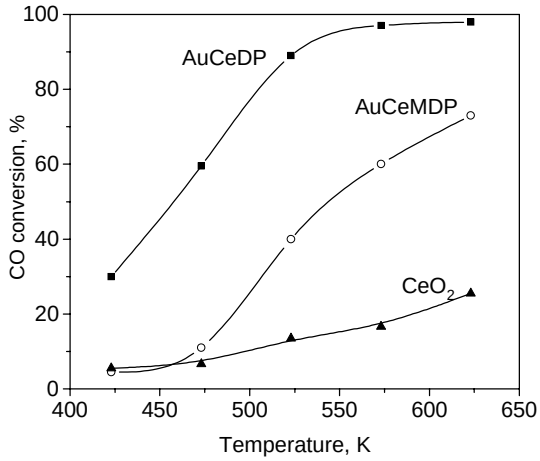

Fig. 1. Temperature dependence of WGS activity (degree of CO conversion) of the samples: (■) AuCeDP; (○) AuCeMDP; and (▲) pure CeO_2.

ture at the reactor outlet was carried out on an "URAS-3G" (Hartmann & Braun AG) gas analyzer with respect to CO and CO_2 content. The catalytic activity was expressed by degree of CO conversion.

3. Results and discussion

Considerable differences are observed in the WGS activity of Au/ceria catalysts. As reported in Fig. 1, the CO conversion over AuCeDP is significantly higher than over AuCeMDP and pure CeO_2 up to 473 K. The activity of ceria remains very low also at higher temperature. It can be suggested that the differences observed in the activity of both gold-containing samples largely arise from the employed preparation methods.

The results reported in the literature reveal that deposition-precipitation is one of the most applicable methods for synthesis of active gold-based catalysts. The deposition-precipitation has advantage, over co-precipitation, to allow preparation of catalysts with narrower particle size distribution where Au is mainly localized on the surface of the supports. Some years ago, some of us employed MDP method for the synthesis of Au/Fe_2O_3 [17]. It was observed that Au/Fe_2O_3 catalyst prepared by this technique exhibited WGS activity higher than the activity of the sample, prepared by co-precipitation. The obtained results have shown that gold dispersion is highly preserved. Moreover, the major part of gold remains on the surface, thus being accessible to catalysis. In this study we compare the activity of catalysts where gold deposition took place either on well-crystallized ceria (DP) or on fully amorphous cerium hydroxide (MDP). In the catalyst prepared by MDP technique, the Ce^{3+} ions act as a reducing agent, converting Au^{3+} to Au^0 still during the preparation procedure, while they themselves are being oxidized to Ce^{4+}. It is known that the catalyst colour is indicative of the proportion of metallic gold; the more metallic gold, the darker the catalyst [13]. The catalyst prepared by MDP method is dark-grey coloured immediately after precipitation of $HAuCl_4$.

HRTEM measurements showed that ceria is highly crystalline in both samples after calcination at 673 K. The analysis of the fringes observed in the micrographs revealed that the support has a cubic structure and that it mainly exposed the (1 1 1) face. Moreover, the presence of very highly dispersed gold clusters (d about 1 nm) in AuCeDP (Fig. 2a) has been evidenced by EDS analysis. In contrast, only large gold particles (average $d \approx 15$ nm) with a lower dispersion have been observed in AuCeMDP (Fig. 2b, the gold particle is marked by a white arrow). EDS analysis revealed that they are gold particles (not shown). In the AuCeDP no gold particles with a larger size or agglomerates of particles like those observed in AuCeMDP have been found. HRTEM images combined with EDS analysis allow us to assume that the gold particles' size in AuCeDP is really very small. The formation of gold particles in Au/ceria catalysts prepared by co-precipitation that are larger than those formed on samples prepared by deposition-precipitation has been reported by other authors [12,14]. Moreover, a significant effect of calcination temperature on the growth of gold particles has been found. On the contrary, the ceria particles size remains unchanged, thus indicating an independent rate of the growth of gold and ceria crystals [12]. We observed similar phenomenon on AuCeMDP. An agglomeration of small metallic gold particles precipitated on freshly prepared $Ce(OH)_3$ takes place during the calcination of the precursor.

The XRD patterns of the samples calcined at 673 K are shown in Fig. 3. They showed the presence of CeO_2 in the cubic crystal structure of fluorite-type, in agreement with HRTEM analysis. The deposition of gold does not influence the size of ceria crystallites. HRTEM measurements and XRD reveal that pure ceria consists of particles with an average size 4.5 nm. Moreover, this size is practically unchanged (4.8 nm) for both Au/ceria catalysts. Recent investigations have revealed that the catalytic activity of gold catalysts supported on ZrO_2, Fe_2O_3–ZrO_2 and Fe_2O_3–ZnO depends strongly not only on the dispersion of gold particles but also on the state and structure of the supports [18]. The authors have concluded that catalytic activity in the WGS is decreased when gold is deposited on amorphous or not well-crystallized support. The differences observed in catalytic activity of gold/ceria catalysts are not connected with the structure of the support, because in both catalysts the ceria support is highly crystalline. On the contrary, pronounced differences in the gold particle size of the samples were observed. No peak related to the presence of gold was discernible in the diffraction pattern of AuCeDP, probably because of the very small size of gold particles. The XRD-pattern for AuCeMDP presented reflection due to crystalline gold at $2\theta = 38.2$. The determination of gold crystallite size based on the diffraction peak broadening according to Sherrer's equation revealed a particles size of about 3.5 nm. The evident disagreement between the sizes

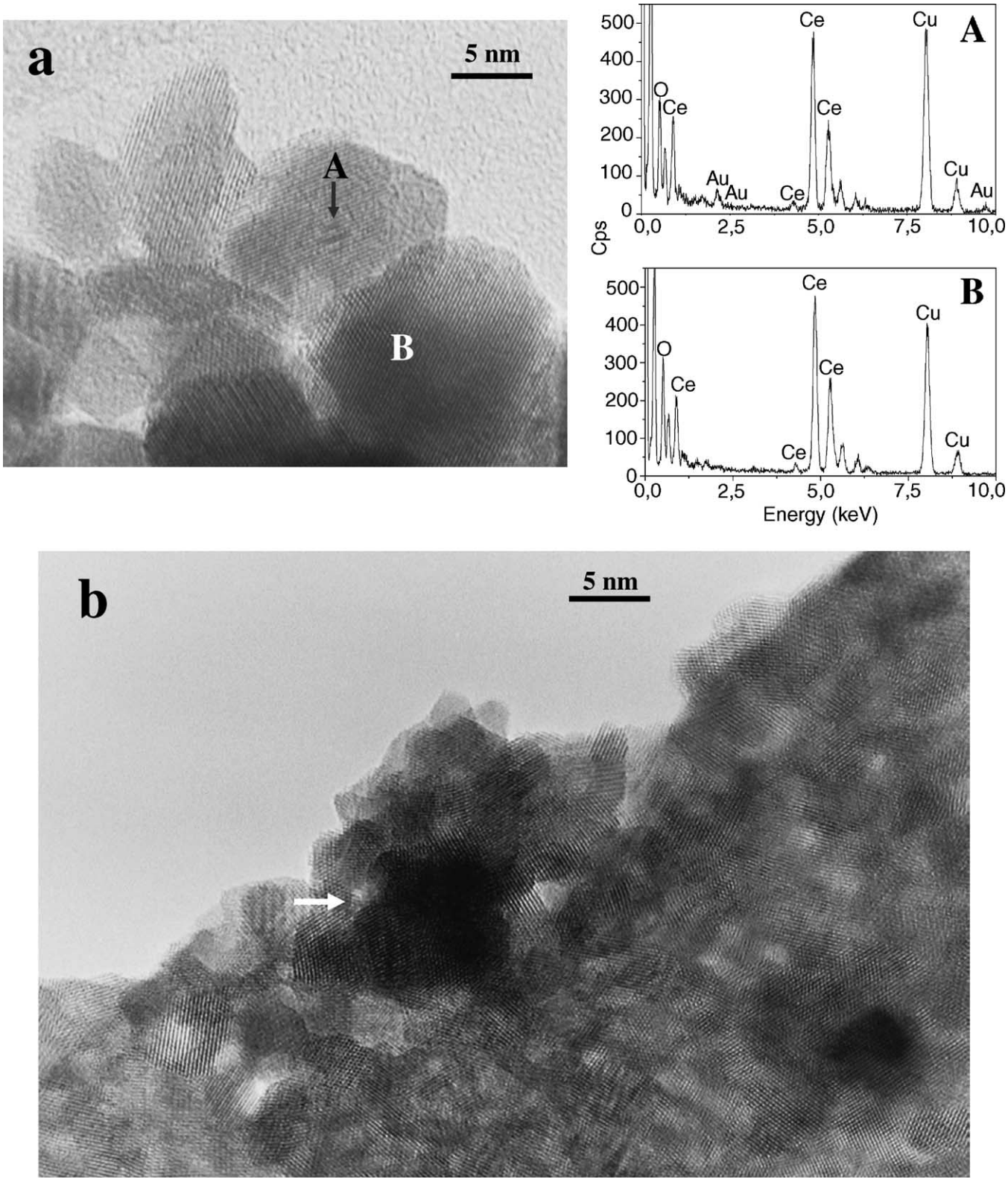

Fig. 2. Section (a): HRTEM image of AuCeDP and EDS analysis in different regions of the same image: (A) ceria and gold nanocluster; (B) ceria alone. The presence of the Cu signal in the EDS spectra is due to the employed grids. Section (b): HRTEM image of AuCeMDP. Both images were taken at an original magnification of 800,000×.

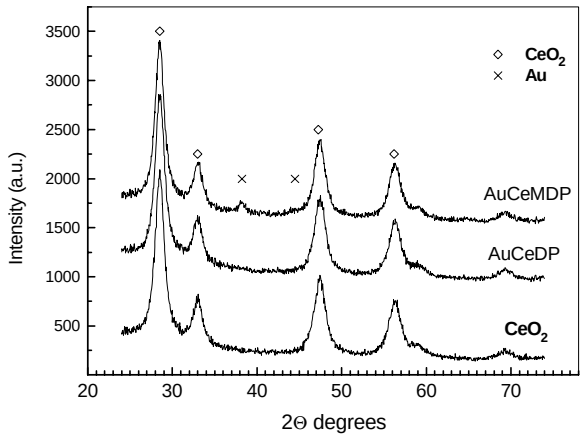

Fig. 3. XRD patterns of Au/ceria catalysts.

of gold particles measured by HRTEM and those calculated by XRD for AuCeMDP sample could be explained taking into account that probably by HRTEM we observe domain or aggregates of gold smaller particles. As it was mentioned above, during the calcination of AuCeMDP small metallic gold particles (that are about 3.5 nm according to XRD) agglomerate to the bigger ones (size about 15 nm) due to the preparation method used.

The XPS data for the O 1s peak of Au/ceria catalysts and of pure ceria are shown in Fig. 4. In all cases, the O 1s peak is complex. Three components in the XPS spectra of fresh (as-prepared) gold-containing samples and initial support could be observed after deconvolution (Table 1). In the XPS spectra of ceria in addition to the lattice oxygen peak (BE = 529.57 eV) a peak is present at BE = 531.73 eV, which is attributed to chemisorbed water and hydroxyls [15]. A component at BE = 534.17 eV could be related to the presence of weakly adsorbed water only on the ceria in oxidized state [19]. In the spectrum of AuCeDP (fresh) catalyst the components at BE = 533.02 and 530.72 eV can be assigned to the weakly adsorbed water and OH^-/CO_3^{2-}, respectively [15,19]. The low energy side of the O 1s binding energy scale (BE = 528.86 eV) corresponds to lattice oxygen and to oxygen ions, all associated with a "2−" formal charge [20]. After reduction of this sample (see Table 1) the peak related to weakly adsorbed water disappears. At the same time the peak assigned to OH^-/CO_3^{2-} decreases significantly. There is no noticeable change in the XPS of O 1s level region of AuCeMDP after reduction. The comparison of the XPS results for both fresh gold/ceria catalysts shows a considerably higher amount of co-ordinated hydroxyl groups and O_2^- on the surface of AuCeDP than on AuCeMDP. Both investigated catalysts have the same gold loading (3 wt.%), but calculated Au surface concentration is 0.69 at.% and 0.20 at.% for both fresh AuCeDP and AuCeMDP, respectively. This result confirms the higher amount of gold exposed on the surface of catalyst prepared by deposition-precipitation (AuCeDP) as a consequence of higher gold dispersion. The slight increase of Au surface

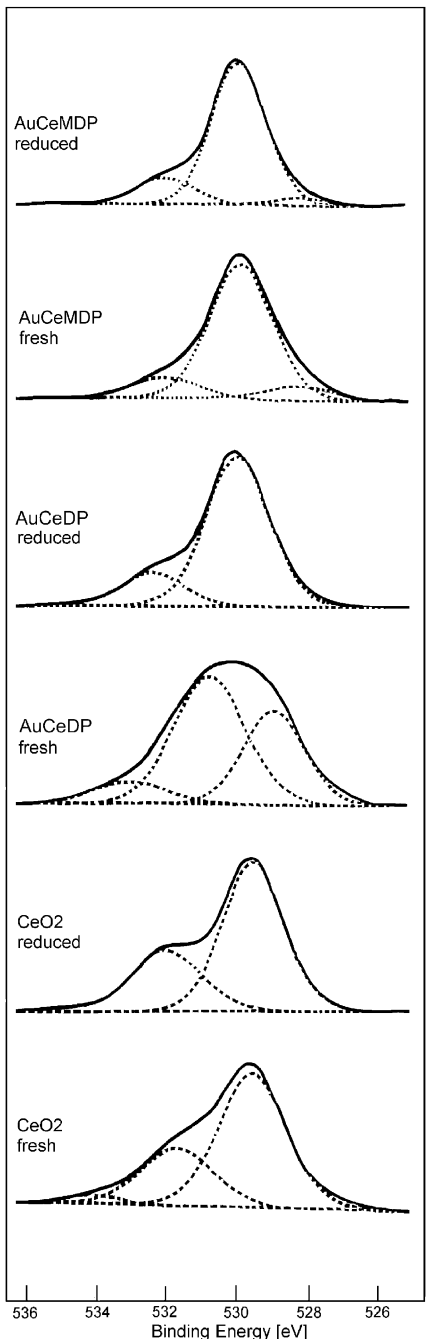

Fig. 4. O1s XP spectra of Au/ceria catalysts.

concentration after reduction (see Table 1) well correlates with FTIR data reported below, which show that the CO adsorption capability of reduced AuCeDP catalyst is increased (see Fig. 6, bold curve). Two peaks due to the Au $4f_{7/2}$ and the Au $4f_{5/2}$ transitions are detected in Au 4f region. In particular, the Au $4f_{7/2}$ peaks is centred at 84.9 and 84.0 eV for AuCeDP and for AuCeMDP, respectively, indicating the presence of gold in metallic state [21]. A difference of BE = 0.9 eV is observed. Such shift has been reported by other authors [22,23] and could be connected with the availability of very small gold clusters on the surface of AuCeDP

Table 1
XPS data for Au/ceria catalysts

Catalyst	Values of O 1s level BE after deconvolution		Au $4f_{7/2}$	Au $4f_{5/2}$	Surface concentration of Au
	BE (eV)	Area (%)	BE (eV)	BE (eV)	at.%
CeO_2 fresh	534.17	3.1			
	531.73	30.2			
	529.57	66.6			
CeO_2 reduced	532.03	31.7			
	529.52	68.3			
AuCeDP fresh	533.02	9.9	84.9	88.6	0.69
	530.72	55.7			
	528.86	34.4			
AuCeDP reduced at 373 K	532.42	17.6	84.6	88.3	0.73
	529.95	82.4			
AuCeMDP fresh	532.02	12.8	84.0	87.6	0.20
	529.77	77.3			
	528.10	9.9			
AuCeMDP reduced at 423 K	531.94	16.5	84.0	87.6	0.12
	529.76	79.5			
	528.07	4.0			

sample. HRTEM and EDS analysis have already shown the presence of very highly dispersed gold clusters ($d \approx 1$ nm) in this sample.

The concentration of Ce^{3+} ions has been calculated from [24]. The estimation of Ce^{3+} concentration evidences that atomic content of Ce^{3+} on the surface of both reduced AuCeDP and AuCeMDP is 0.30 and 0.21, respectively. It is worth noting that on the surface of fresh AuCeDP there is no Ce^{3+}, while on the surface of AuCeMDP the atomic content is 0.16. The higher Ce^{3+} and Au surface concentration on AuCeDP catalyst support the suggestion that on reduced DP sample nanosized metallic gold clusters in close contact with oxygen-vacancy defects of ceria are present and they are responsible for the higher catalytic activity shown by this catalyst [25].

FTIR data confirmed that MDP method applied to gold/ceria catalysts provides condition for preparation of catalyst with larger gold particle size and therefore most part of the gold sites are not exposed at the catalyst surface. The adsorption of CO at 90 K on the oxidized gold/ceria catalysts (Fig. 5) produces a very weak band at 2100 cm^{-1} assigned, on the basis of previous works of gold supported on other oxides [26], to CO chemisorbed on Au^0 step sites of metallic particles. Two bands at 2151 and 2170 cm^{-1} due to CO on Ce^{4+} cations with different co-ordinative unsaturation [27] have been observed on both catalysts, too. Differently from the other previous examined samples and quite unexpectedly, the band at 2100 cm^{-1}, related to CO adsorbed on metallic gold, is very weak in comparison with the intensity observed on gold supported on other oxides. On the basis of a previous study [28], the particles with size of 3 nm are no more covered by oxygen after calcination at 673 K. Only the particles with size smaller than 2 nm are oxidized. The AuCeDP catalyst exhibits high activity in the WGS reaction. Thus, the observed very weak interaction between the gold particles and the CO molecules can suggest that the smallest gold clusters ($d \leq 1$–2 nm) are present on the catalysts surface, but they are covered by oxygen species. As for AuCeMDP, the average gold particles size is 15 nm. These large particles expose only a minimal amount of step sites that are the only ones able to adsorb CO [28].

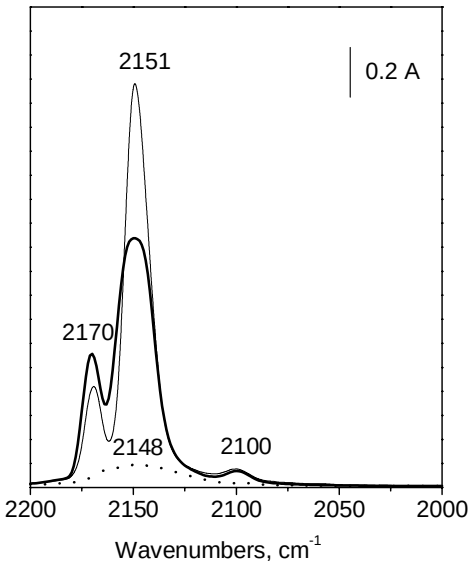

Fig. 5. FTIR absorbance spectra of 2.5 mbar CO adsorbed at 90 K on oxidized samples: AuCeDP (bold curve), AuCeMDP (thin curve) and CeO_2 (dotted curve) in the carbonylic region. All the spectra have been normalised on the weight of the pellets.

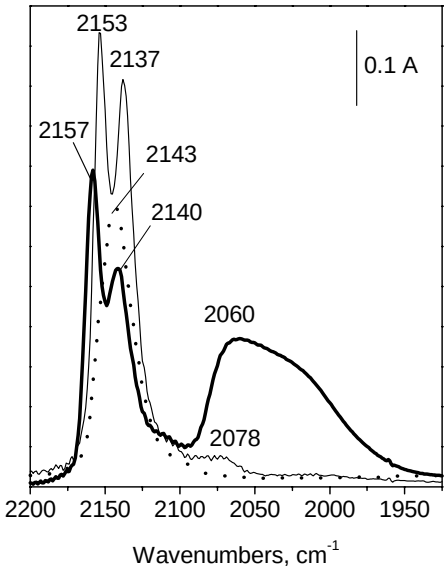

Fig. 6. FTIR absorbance spectra of 2.5 mbar CO adsorbed at 90 K on reduced samples: AuCeDP (bold curve), AuCeMDP (thin curve) and CeO_2 (dotted curve).

Despite the very low intensity of the band at 2100 cm^{-1}, related to CO adsorbed on metallic gold, the presence of gold causes strong modification of ceria on both oxidized samples, which results in appearance of more co-ordinately unsaturated sites on the surface. A weak and broad band at 2148 cm^{-1} is present after CO adsorption at 90 K on pure oxidized CeO_2 (Fig. 5, dotted curve). This band, according to literature data, is due to CO weakly interacting with the Ce^{4+} surface ions. The integrated area of the bands at 2151 and 2170 cm^{-1} is almost the same for both gold/ceria catalysts (35.4 and 34.7 for AuCeDP and AuCeMDP, respectively); while the area of the band at 2148 cm^{-1} is 5.25. Therefore, the increase of intensity of absorption bands of CO on Ce^{4+} observed on both Au/ceria catalysts could be related to a gold-induced modification of the surface properties of ceria.

Adsorption of CO at 90 K on AuCeDP (reduced at 523 K) produced a broad and strong absorption with maximum at 2060 cm^{-1} extending from 2100 to 1950 cm^{-1} (Fig. 6, bold curve). This absorption can be assigned to CO adsorbed on small negatively charged gold clusters with different sizes. The formation of negatively charged gold sites after reduction has already been observed only on fresh Au/α-Fe_2O_3 and Au/TiO_2 catalysts [26]. These very small gold clusters were no more present on used catalysts, probably as a consequence of the sintering of small clusters on TiO_2 and on Fe_2O_3 supports. On the contrary, these features are still present on AuCeDP after many oxidation–reduction treatments and after re-reduction after WGS reaction. This behaviour strongly indicates that the long-term stability of the AuCeDP catalysts is related to high stability of small gold clusters on ceria. In this case, as evidenced by HRTEM and EDS data on the AuCeDP catalyst, a large fraction of the deposited gold is formed by very thin gold clusters covered by adsorbed oxygen at the end of calcination treatment in air. By reduction in H_2, both oxygen adsorbed on the gold clusters and oxygen species on the ceria surface in contact with gold react with hydrogen, giving rise to the formation of water and oxygen vacancies and/or Ce^{3+} defects on ceria. The presence of these defects allows an electron transfer from the support to the gold clusters. The band observed at 2157 cm^{-1} could be assigned to CO adsorbed on Ce^{3+} sites [29]. The band at 2140 cm^{-1} showed a low stability to the outgassing at 90 K and it was not detected at RT. This band corresponds to liquid-like CO [27].

On the contrary, on AuCeMDP (reduced at 523 K) only a very weak and broad band at 2078 cm^{-1} was observed after adsorption of 2.5 mbar CO at 90 K (Fig. 6, thin curve). The integrated area of this band is 1.72, one order of magnitude lower than the integrated area of the band at 2060 cm^{-1} in the spectrum of AuCeDP (18.31). As for the carbonyls on ceria, the integrated area of bands at 2153 and 2137 cm^{-1} observed in the spectrum of AuCeMDP is 17.5, significantly larger than the value obtained for the bands at 2157 and 2140 cm^{-1} on reduced AuCeDP (12.2). This could be an indication of the existence of more free sites on ceria when the gold particles are less dispersed on the surface. These features are also in a good agreement with XPS data showing very low amount of Au sites exposed on the surface.

TPR measurements showed that the surface oxygen of ceria is substantially weakened by the presence of gold [11], its reduction temperature is lowered by several hundred degrees depending on the preparation method, metal loading, calcination temperature. This behaviour has been already observed on other ceria supported catalysts [12–14]. TPR profiles of both gold/ceria catalysts investigated have confirmed that the preparation method influences the surface reduction of ceria and this effect is stronger on catalyst prepared by deposition-precipitation [30]. The peak related to the reduction of surface oxygen of ceria is shifted down to about 390 and 430 K on AuCeDP and AuCeMDP, respectively. It must be stressed that the reduction of the surface capping oxygen of pure ceria occurs at about 770 K [11]. Scire et al. have reported a similar promotional effect of gold on the ceria reducibility for Au/ceria catalysts prepared by deposition-precipitation and co-precipitation [14].

The FTIR spectra collected on AuCeDP, on AuCeMDP and on pure ceria after WGS reaction for 15 min at 473 K are compared in the high frequency range in Fig. 7. A broad band at 2345 cm^{-1} is detected. This band is assigned to gas-phase CO_2 that is produced during the reaction. Bands at 2703, 2812 and 2939 cm^{-1}, related to formate species, can be observed in C–H stretching region in the spectrum of pure ceria (curve 3). These bands are more intense than those observed on AuCeDP (curve 1) and AuCeMDP (curve 2) in the same spectral region. The difference in intensity can be taken as an evidence that the formate species are more stable on bare ceria. On the contrary, on AuCeDP these intermediates are rapidly converted in the reaction products. It has been shown that the decomposition temperature of

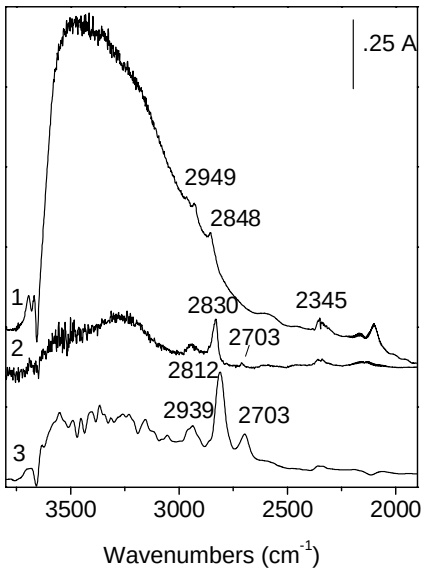

Fig. 7. FTIR spectra recorded after CO–H_2O interaction at 473 K for 15 min on AuCeDP (curve 1); AuCeMDP (curve 2) and on CeO_2 (curve 3).

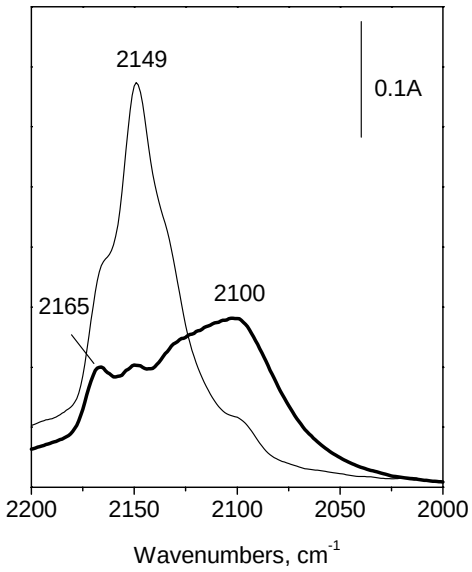

Fig. 8. FTIR absorbance spectra of 4 mbar CO adsorbed on AuCeDP (bold curve) and on AuCeMDP (thin curve) at 90 K after WGS reaction and subsequent outgassing at 373 K.

the formate (450 K) on Rh/CeO_2 is lower than that of the formate on CeO_2 alone (600 K) [31]. Moreover, a band at 2703 cm^{-1} assigned to formyl species is observed in the spectra of pure ceria and of AuCeMDP (very weak). Li et al. [32] have proposed a mechanism involving formyl species as intermediates to explain the formation of formate species after CO adsorption on reduced CeO_2. Formyl species are very unstable and only when the formate species approach their saturation concentration the reverse reaction enables a small amount of formyl to remain on the surface. Thus, the appearance of band related to formyl species can be an evidence for low rate of formate transformation into reaction products on pure ceria and on AuCeMDP. The higher intensity of the bands due to formate species is in agreement with the lower catalytic activity shown by these two samples.

The spectra of 4 mbar of CO adsorbed at 90 K on Au/ceria samples evacuated at 373 K for 15 min after WGS reaction (at 473 K) are shown in the carbonylic region in Fig. 8. Admission of CO on AuCeDP (bold curve) produces bands at 2165 and 2149 cm^{-1}, due to CO on Ce^{4+} and band at 2100 cm^{-1}, already assigned to CO on Au sites. Carbonyls on ceria sites in the spectrum of AuCeDP exhibit reduced intensity as a consequence of the presence of residual formate species and carbonate species on the surface after WGS reaction and subsequent outgassing at 373 K. The blue-shift of the band at 2100 cm^{-1} (Fig. 8, bold curve) previously observed at 2065 cm^{-1} on the reduced sample (see Fig. 6, bold curve) is due to the reoxidation of ceria and consequently to the depletion of negative charge on gold particles under the working conditions [25].

Different features are observed in the spectrum of AuCeMDP (Fig. 8, thin curve). The strong band centred at 2149 cm^{-1} corresponds to CO weakly interacting with the Ce^{4+} surface ions and it could be taken as confirmation that more free surface sites of the support are present on this sample after WGS reaction. Moreover, a similar tendency was observed on freshly reduced catalyst after CO adsorption at 90 K (see Fig. 6, thin curve). However, as it was already shown, this catalyst exhibits lower catalytic activity. Hence, it can be suggested that the existence of more free support surface sites is not a key parameter for WGS activity; it is the availability of well dispersed nano-gold particles located close to the defective ceria surface sites that is indispensable for the high WGS activity.

The gold particles' size is known to have a great influence on the catalytic activity of gold-based catalysts. Goodman and co-workers have found that the specific activity for CO oxidation on model Au/TiO_2 catalyst was extremely sensitive to the gold cluster size with a maximum occurring at ca. 3.2 nm [33]. Our results reveal that both preparation methods lead to the quite different gold particle size. The big differences found in the catalytic activity between two gold/ceria catalysts allow us to confirm that gold particles size is very important factor for the activity. The presence of nanosized gold on the surface of AuCeDP determines its higher WGS activity. Our results are consistent with a study by Scire et al. on the VOC's catalytic combustion of gold/ceria catalysts prepared by deposition-precipitation and co-precipitation [14]. The authors have found that the deposition-precipitation method is more suitable than co-precipitation to obtain highly active Au/ceria catalysts, because DP leads to gold nanoparticles which are preferentially located on the ceria surface. Moreover, low WGS activity and stability of co-precipitated Au/ceria catalyst have been found by Luengaruemitchai et al. [34]. They concluded that the high crystallinity of the ceria in Au/ceria

(1 wt.% Au) negatively affects the activity of the catalyst. The average gold particle size was about 4 nm, on the basis of TEM measurements. Most probably, a very low amount of gold particles on the catalyst's surface seems to be the reason for the above findings.

The comparison of low-temperature WGS activity of Au/CeO_2 prepared by modified deposition-precipitation (this study) and Au/Fe_2O_3 [17] shows the importance of the nature of the supports and of the method of preparation on the catalytic activity of gold catalysts. As it is known, Ce^{3+} ions acts as a reducing agent and by using MDP we can obtain metallic gold particles during the precipitation. The process of thermal treatment at 673 K leads to the crystallization of $Ce(OH)_3$ as nanosized ceria crystallites. At the same time agglomeration of gold particles takes place.

Recent FTIR study on the mechanism of the WGS reaction on gold/ceria catalyst has revealed that reaction proceeds at the boundary between small metallic gold particles and ceria, where CO adsorption on gold and H_2O dissociation on ceria defects take place [25]. The availability of nanosized gold particles on the surface plays a decisive role in explaining the high activity of the catalyst prepared by deposition-precipitation.

4. Conclusions

Structural and catalytic properties in low-temperature WGS reaction have been compared for Au/ceria catalysts prepared by deposition-precipitation and modified deposition-precipitation method. The preparation technique strongly influences catalytic activity due to the large differences in gold particles size and availability of active gold sites at the surface. Deposition-precipitation is more promising method for preparation of active gold/ceria catalysts than modified deposition-precipitation because it allows deposition of bigger part of gold in the form of nanoparticles on the ceria surface. The lower WGS activity of AuCeMDP catalyst could be related to the much larger size of its gold particles and the consequent small amount of gold particles located in close contact with oxygen-vacancy defects of ceria on the catalyst surface, as confirmed by XPS and FTIR data.

Acknowledgements

T.T. would like to thank the CNR—Italy for NATO Outreach Fellowship, which supported FTIR study. T.T., V.I. and D.A. gratefully acknowledge the financial support (project X-1216) by the National Science Fund at the Ministry of Education and Science of Bulgaria.

References

[1] M. Haruta, N. Yamada, T. Kobayashi, S. Iijima, J. Catal. 115 (1989) 301.
[2] M. Haruta, S. Tsubota, T. Kobayashi, H. Kageyama, M.J. Genet, B. Delmon, J. Catal. 144 (1993) 175.
[3] M. Haruta, M. Date, Appl. Catal. A 222 (2002) 427.
[4] T.V. Choudhary, D.W. Goodman, Topics Catal. 21 (2002) 25.
[5] M. Haruta, Cattech 6 (2002) 102.
[6] P. Bera, M.S. Hedge, Catal. Lett. 79 (2002) 75.
[7] Y. Yuan, K. Akasura, A.P. Kozlova, H. Wan, K. Tsai, Y. Iwasawa, Catal. Today 44 (1998) 333.
[8] J.D. Grunwaldt, C. Kiener, C. Wogerbauer, A. Baiker, J. Catal. 181 (1999) 223.
[9] T. Bunluesin, R.J. Gorte, G.W. Graham, Appl. Catal. B 15 (1998) 107.
[10] Y. Li, Q. Fu, M. Flytzani-Stephanopoulos, Appl. Catal. B 27 (2000) 179.
[11] D. Andreeva, V. Idakiev, T. Tabakova, L. Ilieva, P. Falaras, A. Bourlinos, A. Travlos, Catal. Today 72 (2002) 51.
[12] Q. Fu, A. Weber, M. Flytzani-Stephanopoulos, Catal. Lett. 77 (2001) 87.
[13] Q. Fu, Sv. Kudriavtseva, H. Salsburg, M. Flytzani-Stephanopoulos, Chem. Eng. J. 93 (2003) 41.
[14] S. Scire, S. Minico, C. Crisafulli, C. Satriano, A. Pistone, Appl. Catal. B 40 (2003) 43.
[15] L. Armelao, D. Barreca, Surf. Sci. Spectra 8 (2001) 247.
[16] A. Jablonski, B. Lesiak, L. Zommer, M.F. Ebel, H. Ebel, Y. Fukuda, Y. Suzuki, S. Tougaard, Surf. Interface Anal. 21 (1994) 724.
[17] D. Andreeva, T. Tabakova, V. Idakiev, P. Christov, R. Giovanoli, Appl. Catal. A 168 (1998) 9.
[18] T. Tabakova, V. Idakiev, D. Andreeva, I. Mitov, Appl. Catal. A 202 (2000) 91.
[19] Lj. Kundakovic, D.R. Mullins, S.H. Overbury, Surf. Sci. 457 (2000) 51.
[20] J. Dupin, D. Gonbeau, P. Vinatier, A. Levasseur, Phys. Chem. Chem. Phys. 2 (2000) 1319.
[21] J.F. Moulder, W.F. Stickle, P.E. Sobol, K.D. Bomben, Handbook of X-Ray Photoelectron Spectroscopy, Perkin-Elmer, Eden Prairie, 1992, p. 182.
[22] D. van der Putten, R. Zanoni, J. Electr. Spectr. Rel. Phen. 76 (1995) 741.
[23] J. Coulthard, S. Degen, Y.-J. Zhu, T.K. Sham, Can. J. Chem. 76 (1998) 1707.
[24] A. Pfau, K.D. Schierbaum, Surf. Sci. 321 (1994) 71.
[25] T. Tabakova, F. Boccuzzi, M. Manzoli, D. Andreeva, Appl. Catal. A 252 (2003) 385.
[26] F. Boccuzzi, A. Chiorino, M. Manzoli, D. Andreeva, T. Tabakova, J. Catal. 188 (1999) 176, and references therein.
[27] C. Binet, M. Daturi, J.C. Lavalley, Catal. Today 50 (1999) 207.
[28] F. Boccuzzi, A. Chiorino, M. Manzoli, P. Lu, T. Akita, S. Ichikawa, M. Haruta, J. Catal. 202 (2001) 256.
[29] A. Badri, C. Binet, J.C. Lavalley, J. Chem. Soc. Faraday Trans. 92 (1996) 1603.
[30] L. Ilieva, R. Nedyalkova, D. Andreeva, Bulg. Chem. Commun. 34 (2002) 289.
[31] T. Shido, Y. Iwasawa, J. Catal. 141 (1993) 71.
[32] C. Li, Y. Sakata, T. Arai, K. Domen, K. Maruya, T. Onishi, J. Chem. Soc. Faraday Trans. I 85 (1989) 1451.
[33] M. Valden, X. Lai, D.W. Goodman, Science 281 (1998) 1647.
[34] A. Luengaruemitchai, S. Osuwan, E. Gulabi, Catal. Commun. 4 (2003) 215.